

We are IntechOpen, the world's leading publisher of Open Access books Built by scientists, for scientists

4,800

Open access books available

122,000

International authors and editors

135M

Downloads

Our authors are among the

154

Countries delivered to

TOP 1%

most cited scientists

12.2%

Contributors from top 500 universities



WEB OF SCIENCE™

Selection of our books indexed in the Book Citation Index
in Web of Science™ Core Collection (BKCI)

Interested in publishing with us?
Contact book.department@intechopen.com

Numbers displayed above are based on latest data collected.
For more information visit www.intechopen.com



Wave Iterative Method for Electromagnetic Simulation

Somsak Akatimagool and Saran Choocadee

Additional information is available at the end of the chapter

<http://dx.doi.org/10.5772/51450>

1. Introduction

Presently, the microwave circuit design is the most critical and necessary for modern communication systems. The problems with the design of circuits often include a lack of equipment and tools used to design and build them. Numerical methods related to electromagnetic waves have caused a revolution in microwave engineering; techniques such as FDTD (Finite Differential Time Domain) [1], TLM (Transmission Line Matrix) [2], and the Moment method [3] have been developed. Each method has respective disadvantages and limitations of usage for both research and education. To perform the electromagnetic wave analysis of waveguide structures, several classic approaches can be found in the literature. A practical example of computer aid design is that the inductive iris in a rectangular waveguide has been analyzed with high accuracy through approximate modeling utilizing the full wave Mode Matching Method (MMM) [4] and Transmission Line Matrix (TLM) [5]. Therefore, the development and optimization of numerical methods are important for an efficient electromagnetic simulation tool [6-7].

In this chapter, we study and introduce an efficient electromagnetic simulation tool for analysis of inductive and capacitive obstacles and rectangular window in waveguides. The Wave Iterative Method (WIM) based on iterative procedure and wave propagation theory is proposed. This method has been combined with mode matching technique to characterize the obstacle in a rectangular waveguide. Also, the compact CAD tool and presenting the electromagnetic field distributions included in this topic.

2. Wave propagation and waveguide

Several years ago, the characteristics of waves in source-free, homogeneous regions of space have been discussed. Accordingly, we present this section by considering the reflection,

transmission and incident experienced by electromagnetic waves on stratified dielectric surface.

There are many situations where a wave passes through several layers of different materials. One example is the passage of electromagnetic through a free space with transmission line mode or TEM. There are several ways use to analyze the correct results, but a very common method is an impedance transformation that integrates reflections into a single parameter to generate the numerical results.

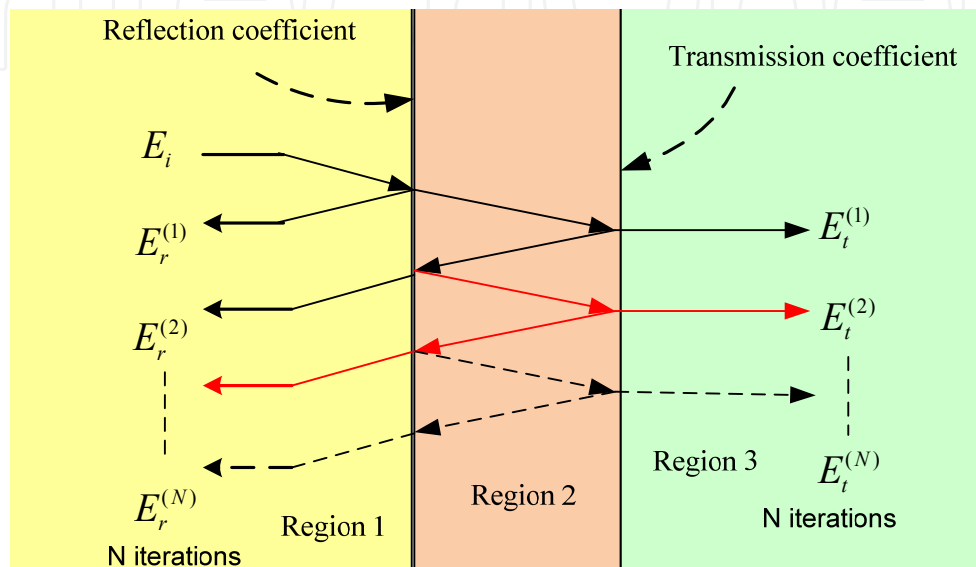


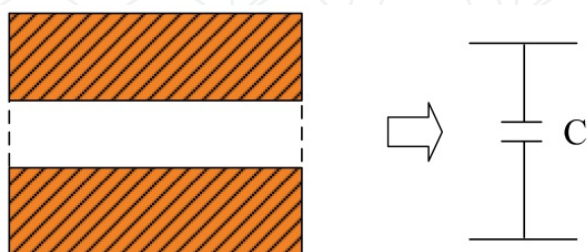
Figure 1. (a) The wave propagation in stratified interface

Fig.1 shows a stratified dielectric region. When a wave is normally incident from the region 1 and transmitted into region 2 and region 3 respectively, an infinite number of transmitted, reflected waves in the same wavelength are produced at the boundary interface. At a time, the all incident waves (E_i), reflected waves (E_r) and transmitted waves (E_t) can be considered to be a single of each wave. We can develop the reflection coefficient expression by following the progression of the incident waves and its reflections. Similarly, the transmission coefficient expression can be presented by following the progression of the incident wave and its transmissions. Finally, we can use the relationship of expressions to calculate the properties of boundary interface.

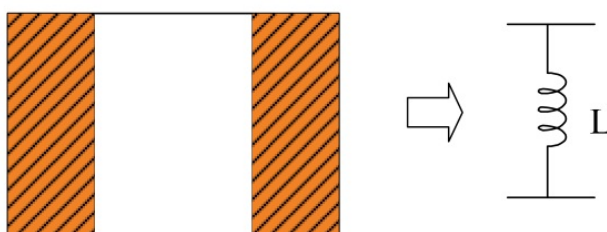
Waveguides are used to transport electromagnetic energy along a fixed path that carries non-TEM modes, often called waveguide modes. Most important of waveguide properties is that they can support an infinite number mode of filed generated by diffraction form each interface within waveguide [8]. Waveguides are almost operated so that only a single propagation mode is present because the presence of more than one propagating mode causes dispersion. Typically, they must be operated over smaller bandwidths and smaller losses than transmission line, which makes them attractive for many applications. One of several examples is to place obstacle element in waveguides to make devices such as lumped element, filters, couplers or antenna. Fig.2(a) shows two thin metal fins placed on

the top and bottom walls of a waveguide, called a capacitive window. Considering in the gap of obstacle, when the electric field within the window increases, the energy stored between two conducting surfaces will increase. We observed that the equivalent circuit of obstacle is a shunt capacitor.

Similarly, Fig.2(b) shows an inductive window which the most magnetic fields can flow through in the obstacle width. The equivalent circuit of obstacle is a shunt inductor.



(a) capacitive window



(b) inductive window

Figure 2. (a) The capacitive and inductive windows

3. Wave iterative method (WIM)

An analysis of the electromagnetic wave properties within a waveguide consists of TE and TM field components. Most wave analyses are calculated in the spectral domain based on the series integration equation to present the electromagnetic field and to analyze the two ports network parameters such that the result of the frequency response reflects the characteristic of various planar circuits. In this section, we will present the cooperation of waves between the real domain and the spectrum domain.

The calculating concept for the electromagnetic wave propagation in a waveguide is based on the Wave Iterative Method (WIM) [9-11]. The operating process, as shown in Fig.3, present the amplitude and direction of the incident, reflected, and transmitted waves what propagate in the waveguide obstacle. On the obstacle, the waves are calculated in the real domain (pixels) and the waves in the free space are calculated in the spectrum domain (modes). To alternate between both domains, we use the Fast Fourier Transform (FFT) to reduce the computation time and show directly the electromagnetic field in the real domain.

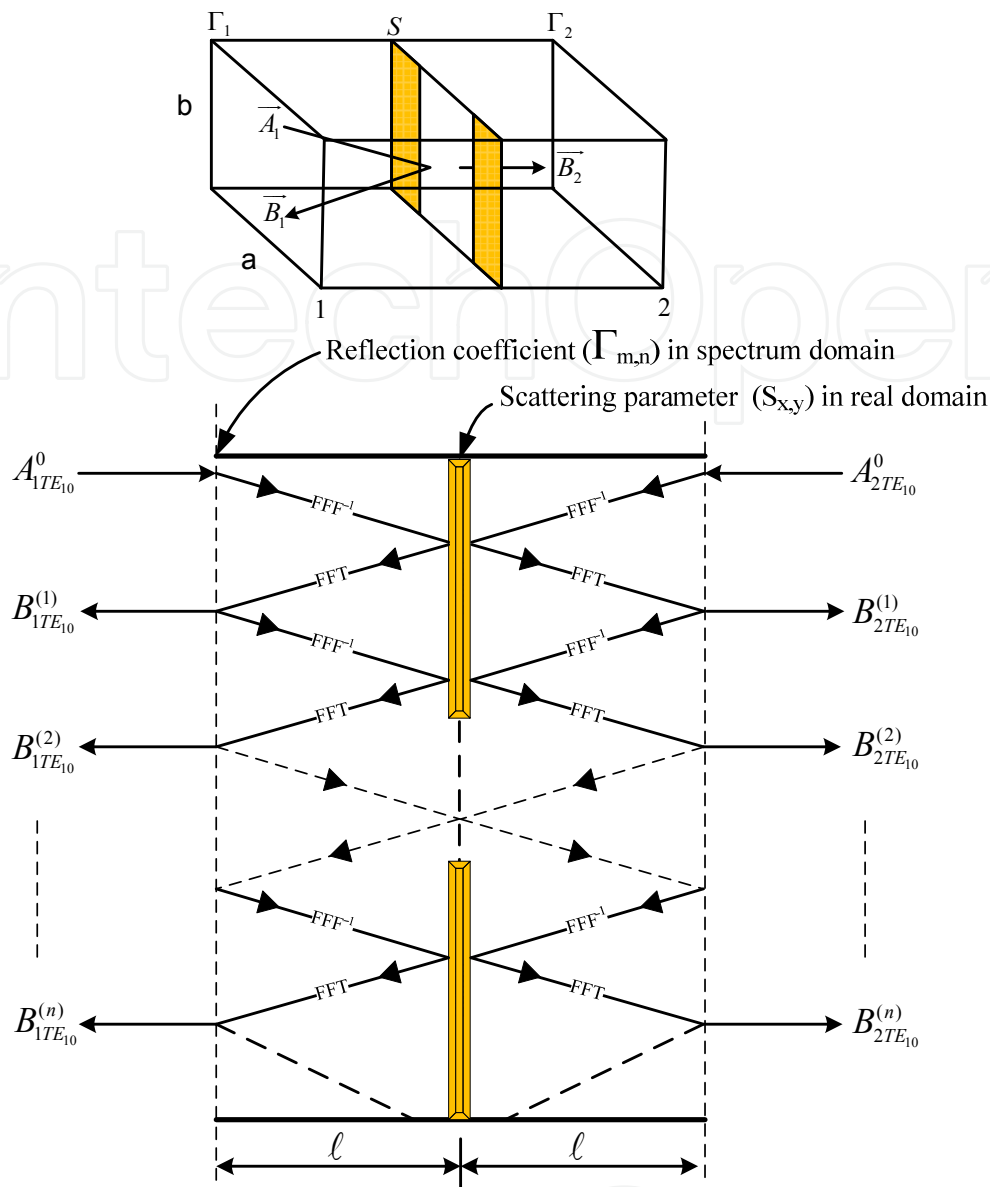


Figure 3. (a) The wave propagation in the waveguide

In Fig.3, the first step, the TE₁₀ field which is the dominant mode, propagate into the obstacle as iris circuit, and then the higher-mode waves caused by the scatter on the conductor surface will be incident and will reflect within the waveguide. An infinite numbers of reflected and transmitted waves are produced at the obstacle interface. Finally the calculation of waves will use the principle of mode matching at the input and the output ports of the waveguide.

The initial value of dominant mode, TE_{1,0} is

$$A_{x,y}^{(0)} = -\sqrt{\frac{2}{ab}} \sin\left(\frac{\pi x}{a}\right), \quad (1)$$

where a and b are the dimension of the waveguide. The reflected waves $(B_{x,y})$ in n^{th} iteration on the obstacle are

$$B_{x,y}^{(n)} = S_{x,y} A_{x,y}^{(n-1)}. \quad (2)$$

The scattering parameter $(S_{x,y})$ of waves in the real domain for a two-port network is defined as

$$[S_{x,y}] = \begin{bmatrix} -S_{C(x,y)} & S_{D(x,y)} \\ S_{D(x,y)} & -S_{C(x,y)} \end{bmatrix}, \quad (3)$$

where S_C is equal to 1 in the conductor area and S_D is equal to 1 for the free space. To transform the wave from the real domain to the spectrum domain, we use the Fast Fourier Transform (FFT) of the TE/TM modes as

$$B_{m,n}^{(n)} = \text{Modal_FFT}(B_{x,y}^{(n)}). \quad (4)$$

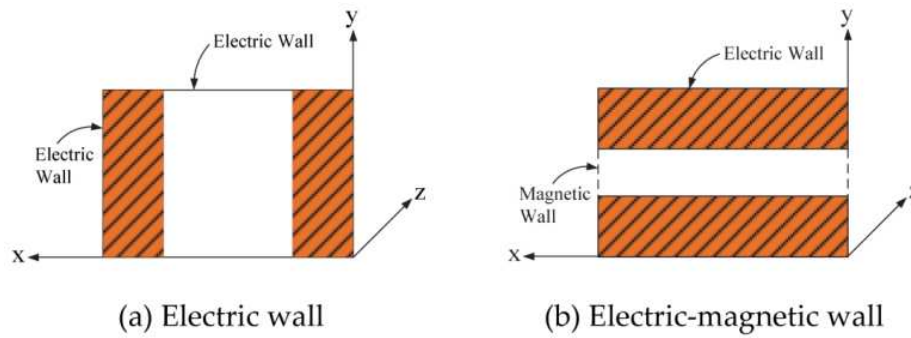


Figure 4. The electric and magnetic walls around the waveguide

The basic functions of TE field components in the electric wall [12], as shown in Fig.4(a) for an inductive obstacle, are

$$\bar{E}_{x(x,y)}^{\alpha} = K_x^{\alpha} \cos\left(\frac{m\pi x}{a}\right) \sin\left(\frac{n\pi y}{b}\right), \quad (5)$$

$$\bar{E}_{y(x,y)}^{\alpha} = -K_y^{\alpha} \sin\left(\frac{m\pi x}{a}\right) \cos\left(\frac{n\pi y}{b}\right), \quad (6)$$

where α refers to the TE mode and K is the constant value with respect to the x and y directions. The equations are defined as

$$\begin{aligned} K_x^{TE} &= \frac{n\sqrt{\frac{2\tau}{ab}}}{b\sqrt{\frac{m^2}{a^2} + \frac{n^2}{b^2}}}, & K_x^{TM} &= \frac{m\sqrt{\frac{2\tau}{ab}}}{a\sqrt{\frac{m^2}{a^2} + \frac{n^2}{b^2}}} \\ K_y^{TE} &= \frac{-m\sqrt{\frac{2\tau}{ab}}}{a\sqrt{\frac{m^2}{a^2} + \frac{n^2}{b^2}}}, & K_y^{TM} &= \frac{n\sqrt{\frac{2\tau}{ab}}}{b\sqrt{\frac{m^2}{a^2} + \frac{n^2}{b^2}}} \end{aligned} \quad (7)$$

where $\tau = 1$ if $m, n = 0$ and $\tau = 2$ if $m, n \neq 0$.

The basic functions of TM field components in the electric-magnetic wall [12], as shown in Fig.4(b) for a capacitive obstacle, are

$$\bar{E}_{x(x,y)}^\alpha = -K_x^\alpha \sin\left(\frac{m\pi x}{a}\right) \sin\left(\frac{n\pi y}{b}\right), \quad (8)$$

$$\bar{E}_{y(x,y)}^\alpha = K_y^\alpha \cos\left(\frac{m\pi x}{a}\right) \cos\left(\frac{n\pi y}{b}\right), \quad (9)$$

where α refers to the TM mode and K is the constant value respect to the x and y directions. The equations are defined as

$$\begin{aligned} K_x^{TE} &= \frac{n\sqrt{\frac{2\tau}{ab}}}{b\sqrt{\frac{m^2}{a^2} + \frac{n^2}{b^2}}}, & K_x^{TM} &= \frac{m\sqrt{\frac{2\tau}{ab}}}{a\sqrt{\frac{m^2}{a^2} + \frac{n^2}{b^2}}} \\ K_y^{TE} &= \frac{m\sqrt{\frac{2\tau}{ab}}}{a\sqrt{\frac{m^2}{a^2} + \frac{n^2}{b^2}}}, & K_y^{TM} &= \frac{-n\sqrt{\frac{2\tau}{ab}}}{b\sqrt{\frac{m^2}{a^2} + \frac{n^2}{b^2}}} \end{aligned} \quad (10)$$

where $\tau = 1$ if $m, n = 0$ and $\tau = 2$ if $m, n \neq 0$.

At the input port of the waveguide, the incident waves ($A_{x,y}$) of higher-order modes will feedback into the obstacle of the waveguide. The equation for incident waves ($A_{m,n}$) is

$$A_{m,n}^{(n)} = \Gamma_{m,n} B_{m,n}^{(n)} + A_{1,0}^{TE/TM}, \quad (11)$$

where $A_{1,0}$ is an initial exciton source. The reflection coefficient ($\Gamma_{m,n}$) of waves in the spectrum domain at the input and the output ports of the waveguide can be written as

$$\Gamma_{m,n} = \Gamma_{m,n}^{TE/TM} = \frac{1 - Z_0 Y_{m,n}^{TE/TM}}{1 + Z_0 Y_{m,n}^{TE/TM}}, \quad (12)$$

where Z_0 is the intrinsic impedance of the dominant mode and $Y_{m,n}^{TE/TM}$ is the TE/TM modes admittance with the orders of m and n which can be expressed as

$$Y_{m,n}^{TE} = \frac{\left(\frac{m\pi}{a}\right)^2 + \left(\frac{n\pi}{b}\right)^2 - \omega^2 \mu \epsilon}{j\omega\mu}, \quad (13)$$

$$Y_{m,n}^{TM} = \frac{j\omega\epsilon}{\left(\frac{m\pi}{a}\right)^2 + \left(\frac{n\pi}{b}\right)^2 - \omega^2 \mu \epsilon}. \quad (14)$$

Therefore, considering the waves on the obstacle, the waves ($A_{m,n}$) will be transformed by using the Inverse Fast Fourier Transform (IFFT) to analyze the basic functions of TE/TM field components by using Eq.(5)-(8), to come back to the real domain as

$$A_{x,y}^{(n)} = \text{Pixel_IFFT}\left(B_{m,n}^{(n)}\right). \quad (15)$$

The implementation of the Wave Iterative method consists of a recurrence relationship of wave between the propagation in both sides of the waveguide and the propagation on the obstacle. From Eq.(2) and Eq.(11), the total waves at n^{th} iteration are

$$A_{m,n}^{(n)} = \Gamma_{m,n} \hat{S} A_{m,n}^{(n-1)} + A_{1,0}^{TE/TM}, \quad (16)$$

where \hat{S} is the spectrum operator of scattering coefficient.

Considering the wave propagation in the rectangular waveguide with zero thickness obstacles, the electromagnetic equivalent circuit of the obstacle section is presented to identify the impedance (Z) element and the input and the output sections of the waveguide are presented by dominant mode admittance, as shown in Fig.5.

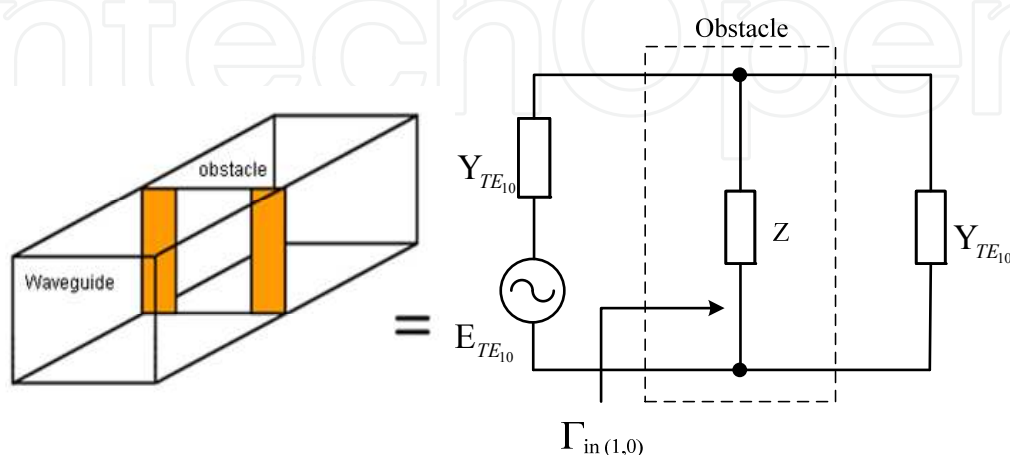


Figure 5. (a) The electromagnetic equivalent circuit of an obstacle

At the convergence condition, the reflected wave on the obstacle at n^{th} iteration, is tend toward zero, the total waves will be the steady state field. So, we can obtain the input reflection coefficient of obstacle circuit of dominant mode , $\Gamma_{in(1,0)}$ as,

$$\Gamma_{in(1,0)} = \frac{B_{1,0}^{TE/TM}}{A_{1,0}^{TE/TM}} = \frac{\sum_{n=1}^N B(n)_{1,0}^{TE/TM}}{A_{1,0}^{TE/TM}}. \quad (17)$$

The input impedance, $Z_{in(1,0)}$ of zero thickness obstacles in the rectangular waveguide can be written as

$$Z_{in(1,0)} = Z_0 \left(\frac{\Gamma_{in(1,0)} - 1}{2\Gamma_{in(1,0)}} \right). \quad (18)$$

Then, the input reactance will be a positive imaginary value for an inductive element and a negative imaginary value for a capacitive element. If the input impedance is equal to zero or infinity, the obtained element will be a LC series or parallel resonant circuit respectively. The net 2.5D electric field distribution on the obstacle by summing the amplitude of the incident and the reflected waves of N iterations can be expressed as

$$E_{x,y} = \sqrt{Z_0} \sum_{n=1}^N \left(A_{x,y}^{(n)} + B_{x,y}^{(n)} \right). \quad (19)$$

Similarly, the net 2.5D magnetic fields can be expressed by subtracting the amplitude of the incident and the reflected waves of N iterations series as can be expressed as

$$H_{x,y} = \frac{1}{\sqrt{Z_0}} \sum_{n=1}^N \left(A_{x,y}^{(n)} - B_{x,y}^{(n)} \right). \quad (20)$$

4. WCD simulation design

In this topic, we present a developed simulation program that conducts a numerical analysis by using the Wave Iterative Method (WIM), shown in the Fig.6. This developed simulation program, called WCD (Waveguide Circuit Design), consists of a main menu, parameter setup, and a design and display window, as shown in Fig.7. The WCD is constructed by using the GUI (Graphic User Interface) of MATLAB®. The user can setup the initial values that are used for calculating of the two ports network, calculate the obstacle characteristics and select the display windows of the simulated results. With the simulation program, it is possible to analyze and design the waveguide iris, waveguide filter and also visualize the 2.5D electromagnetic field distribution.

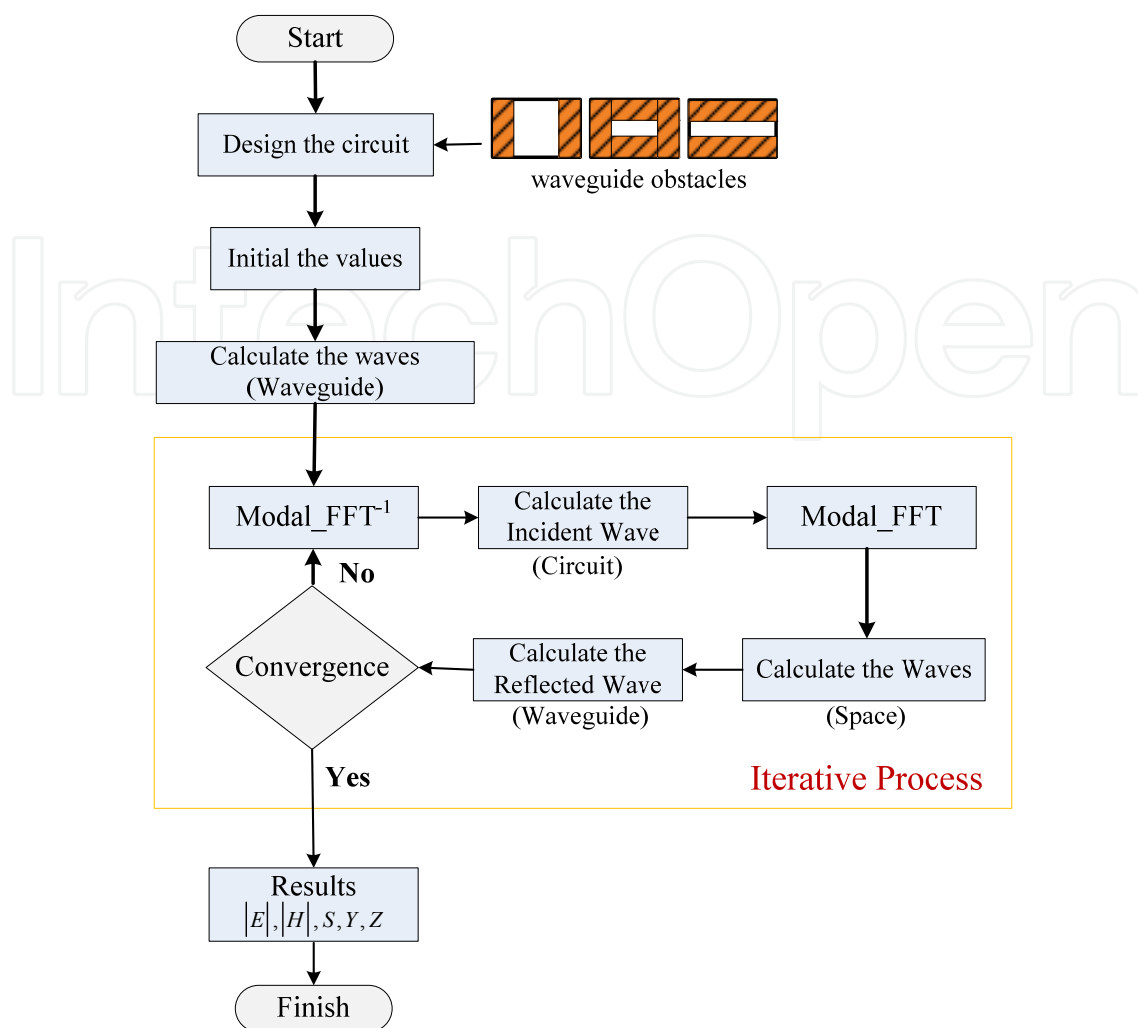
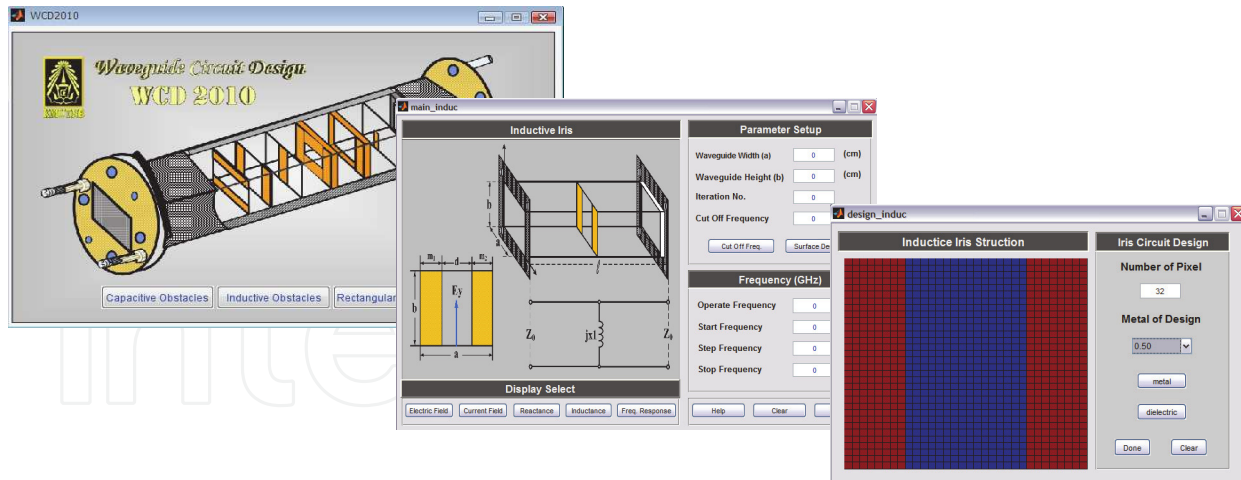


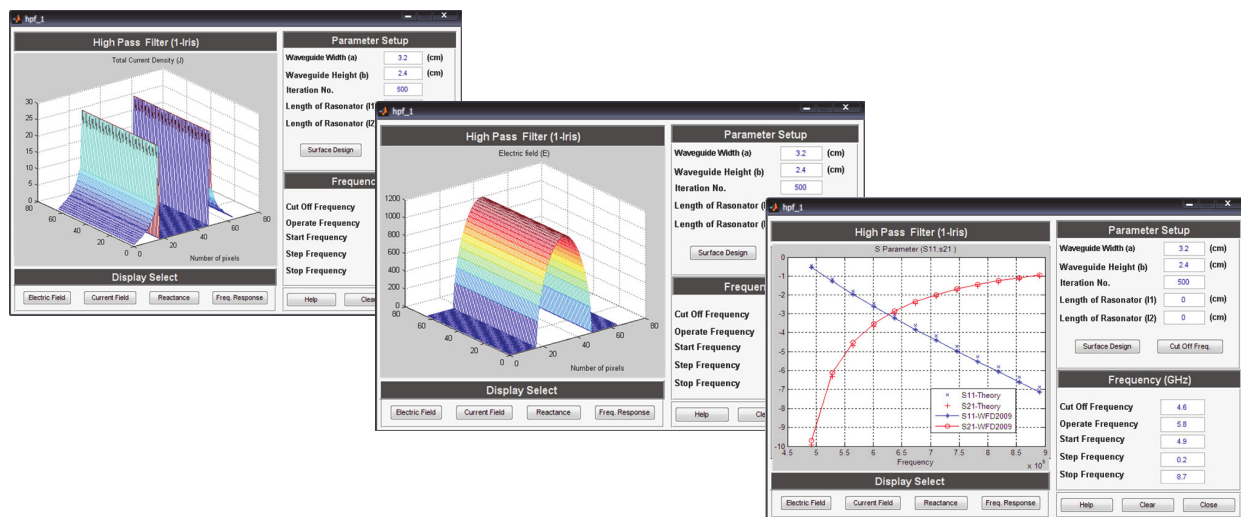
Figure 6. Flowchart of WCD simulated process

The simulated process of the WCD, as shown in Fig.6, is following:

1. Start the simulation program from the main menu which consists of an inductive, a capacitive and a window obstacle bottom, as shown in Fig.7 (a).
2. Design the waveguide obstacle structure what the user can determinate the desired obstacle dimensions, as shown in Fig.7(a).
3. Set the initial values; such as the size, length, frequency operating, dielectric constant, etc., as shown in Fig.7(a).
4. Calculate the incident wave of the dominant mode.
5. Calculate the reflected and the transmitted waves on the obstacle surface in the real domain and in the free space in the spectrum domain. In this process, an infinite number of the transmitted and the reflected waves are produced on the obstacle interface. However the reasonable numbers of iteration are determined, the process will result in termination.
6. Present the simulated results; such as the electric and the magnetic field distribution, the impedance, the scattering and the admittance parameters, as shown in Fig.7(b).



(a) Menu and parameter setup windows



(b) Display windows

Figure 7. Waveguide Circuit Design (WCD) Tool

5. Simulation results

In this chapter, we present the analysis of the inductive, the capacitive obstacles and the rectangular window in the waveguide by using the developed WCD simulation and also introduce the electromagnetic distribution in the waveguide. The simulated WCD results will be compared with the CST simulation.

5.1. Inductive obstacle analysis

The vertical obstacle section transforms the inductive equivalent circuit, shown in Fig.8. The dimensions of rectangular waveguide consists of a width (a) equal to 6.4 cm., a height (b) equal to 3.2 cm. and the usable obstacle width (d) equal to 3.2 cm. and 4 cm. respectively. The cutoff frequency of the waveguide is 3.24 GHz.

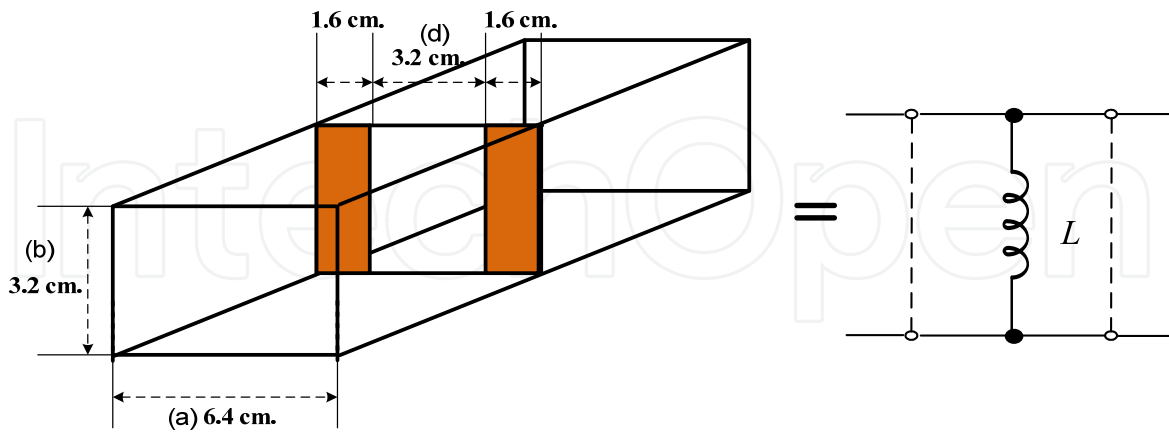


Figure 8. (a) Inductive obstacle structure

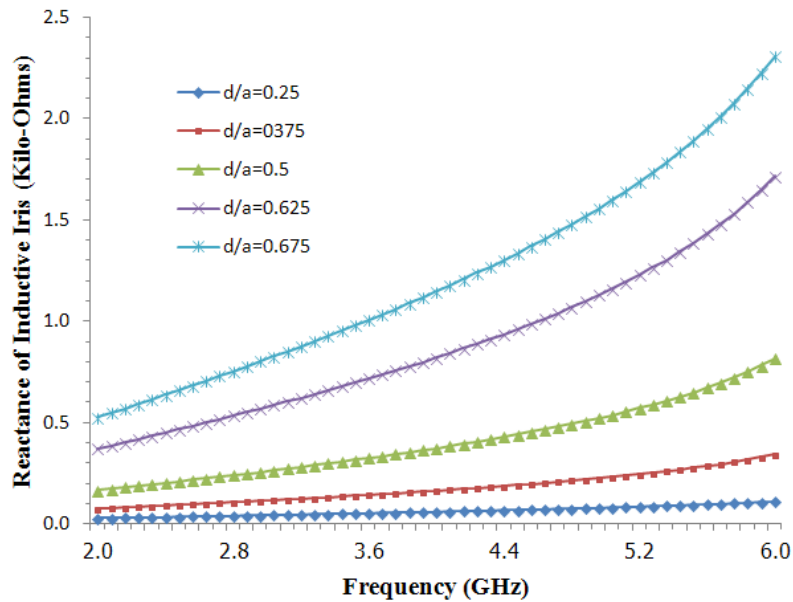


Figure 9. The inductance of inductive obstacle

Fig.9 presents the input reactance of the inductive obstacle in frequency range from 2-6 GHz following the variation the ratio of obstacle and the waveguide width. We observed that the obstacle width increased, the reactance of the inductive obstacle will increase that is consistent with the properties of the inductor.

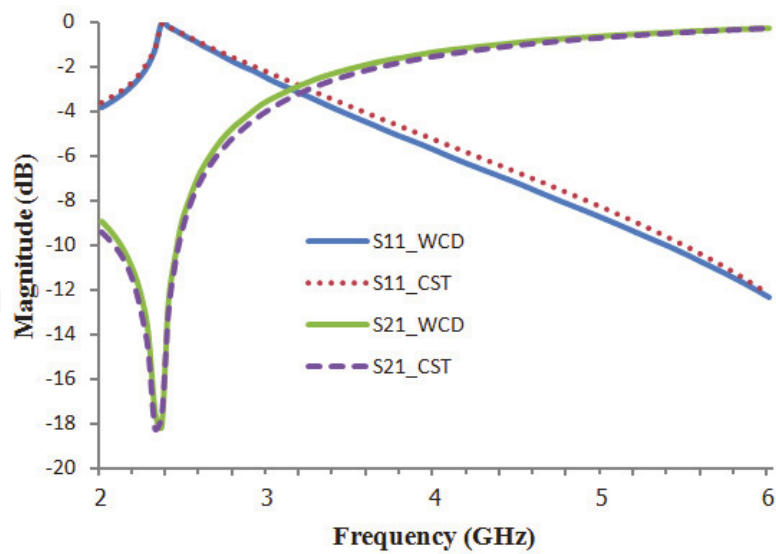
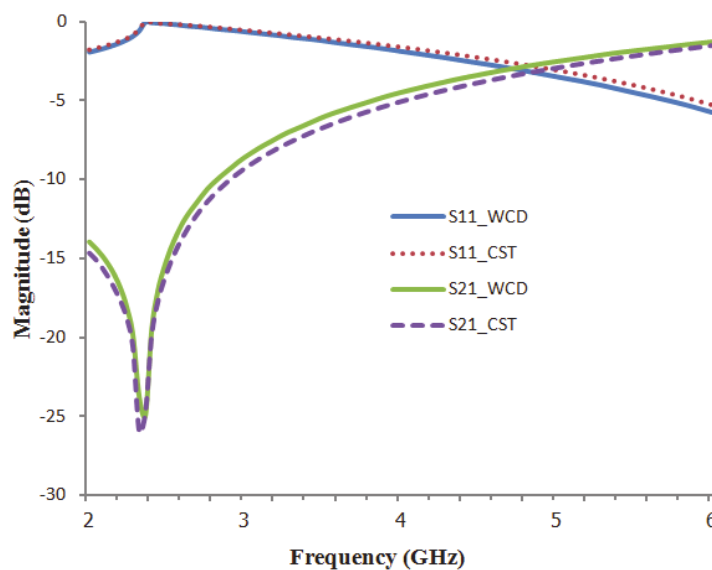
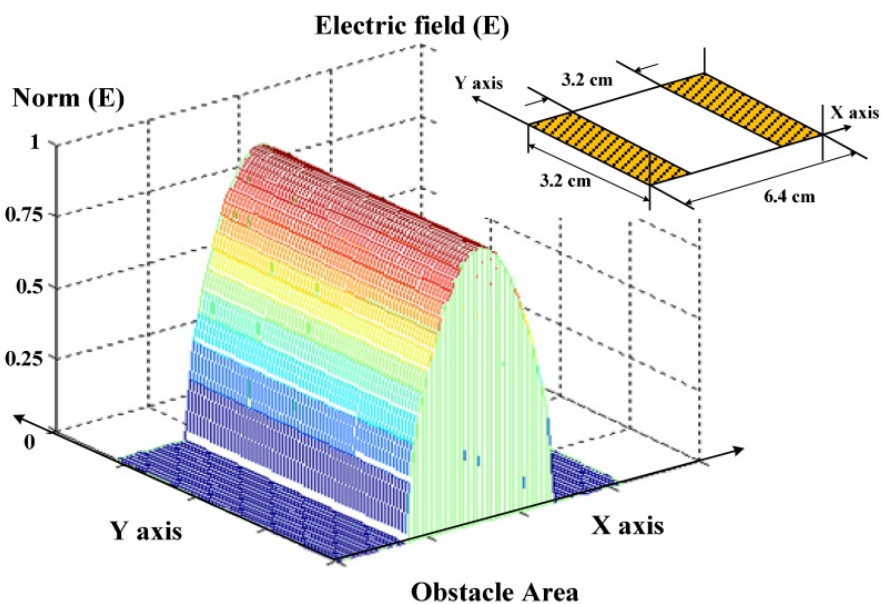
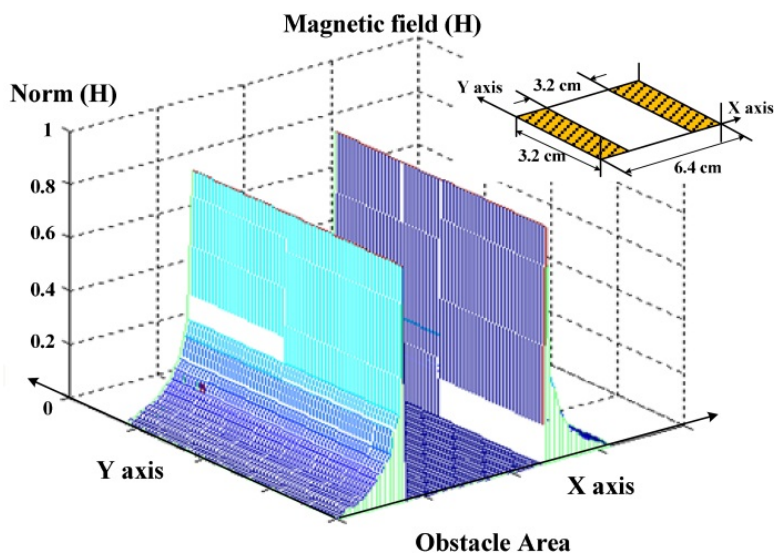
(a) Obstacle structure ratio of $d/a = 0.5$ (b) Obstacle structure ratio of $d/a = 0.375$

Figure 10. Comparison of dB(S11), dB(S21) of the inductive obstacle between the WCD and the CST simulation

Fig.10(a) presents the comparison of dB(S11) and dB(S21) of the inductive obstacle structure between the WCD and the CST simulation. In the case of an obstacle width equal to 3.2 cm., we can obtain the -3 dB cutoff frequency at 3.15 GHz. and Fig.10(b) presents the comparison of dB(S11) and dB(S21) of the inductive obstacle structure between the WCD and the CST simulation, at an obstacle width equal to 4.0 cm. We can obtain the -3 dB cutoff frequency at 4.78 GHz. This comparison revealed good agreement. We observed that the shunt inductive circuit is presented as a high pass filter.



(a) Electric field



(b) Magnetic field

Figure 11. The 2.5D electromagnetic field illustration

Fig.11 shows the 2.5D normalized electromagnetic field distributions on the inductive obstacle that are agreements with the electromagnetic field theory. The electric field density of TE₁₀ fundamental mode, as shown in Fig.11(a) is maximum at the center obstacle and is minimum at the discontinuity of boundary obstacle. We observed that the electric field on the conducting surface is null. In Fig.11 (b), the amplitude of magnetic field on discontinuity of boundary obstacle is peak, and decreases until to zero following the distance on the both sides of the conductor.

5.2. Capacitive obstacle analysis

The horizontal obstacle section transforms the capacitive equivalent circuit, shown in Fig.12. The dimensions of rectangular waveguide consists of a width (a) equal to 6.4 cm., a height (b) equal to 3.2 cm., and the obstacle of iris circuit equal to 0.8 cm. and 0.4 cm. respectively.

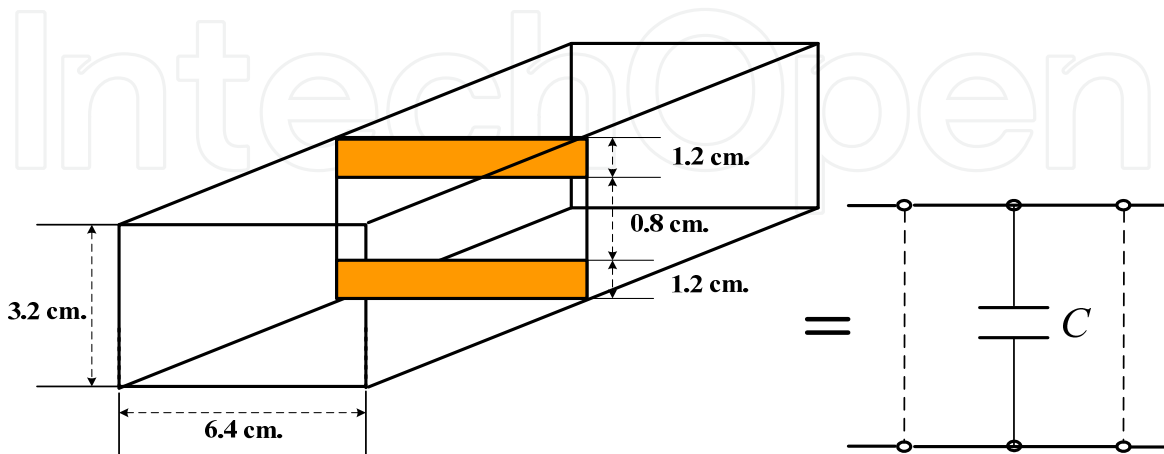


Figure 12. (a) Capacitive obstacle structure

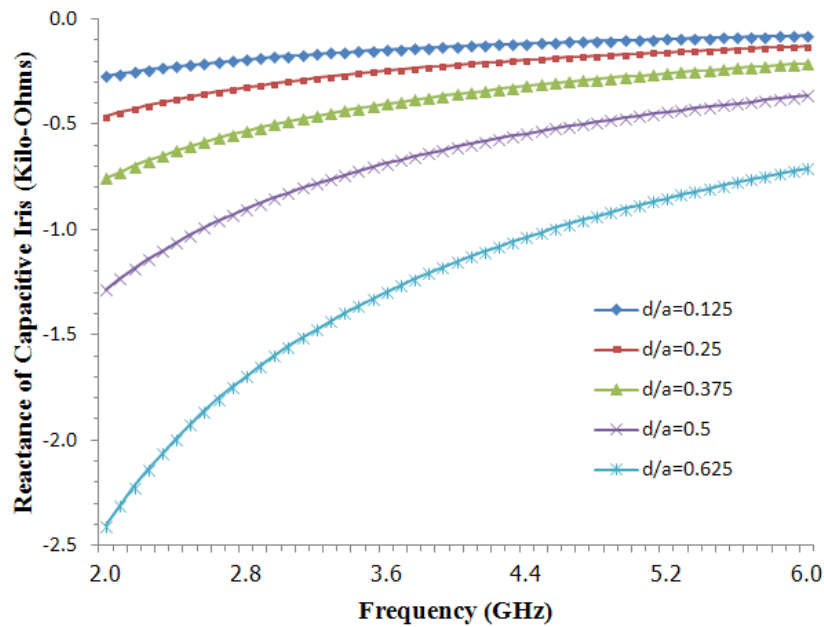


Figure 13. The capacitance of capacitive obstacle

Fig.13 presents the input reactance of the capacitive obstacle in frequency range from 2-6 GHz following the variation the ratio of obstacle and waveguide width. We observed that the obstacle width increased, the reactance of the capacitive obstacle will increase that is consistent with the properties of the capacitor.

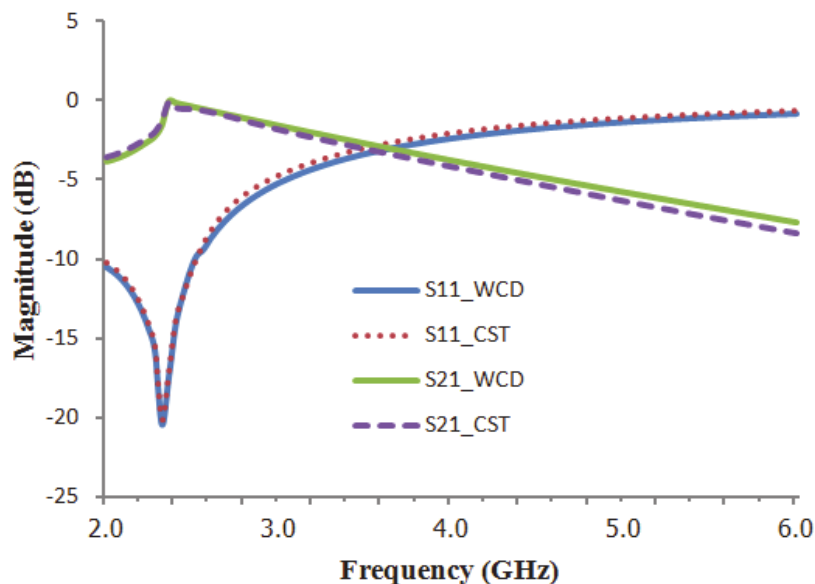
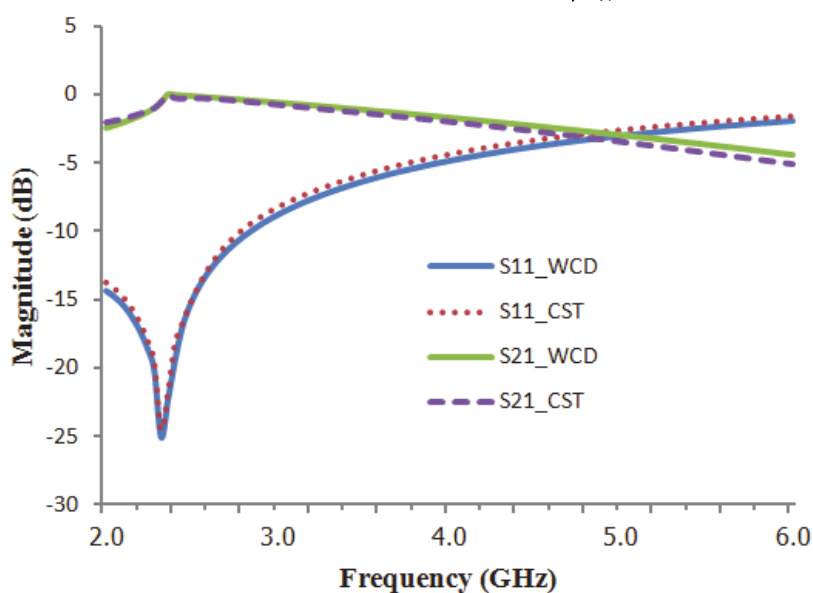
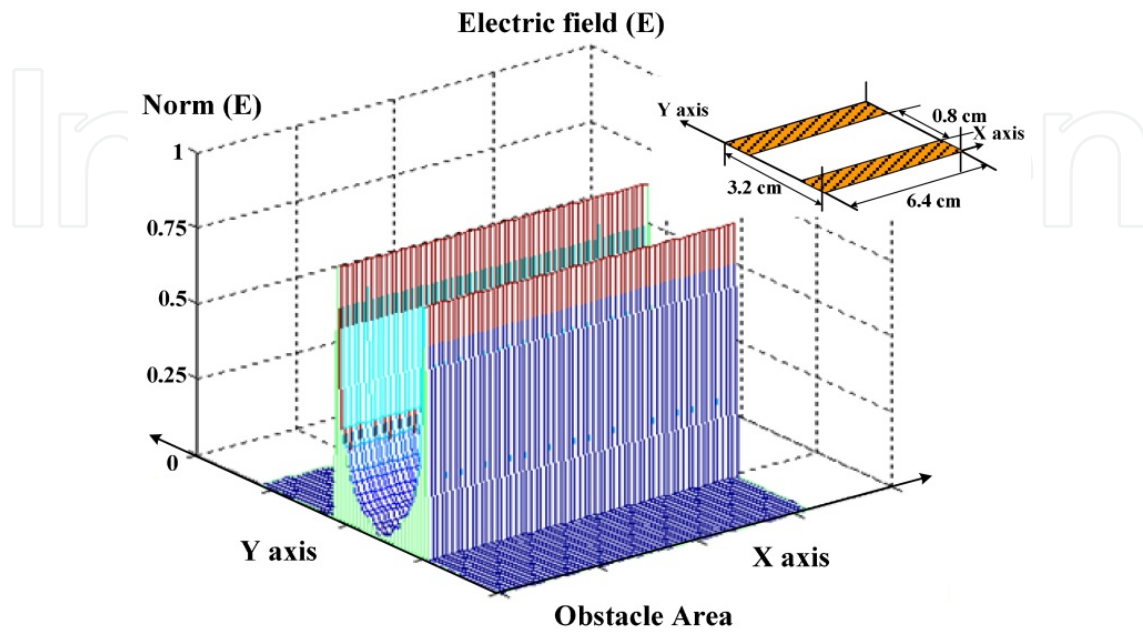
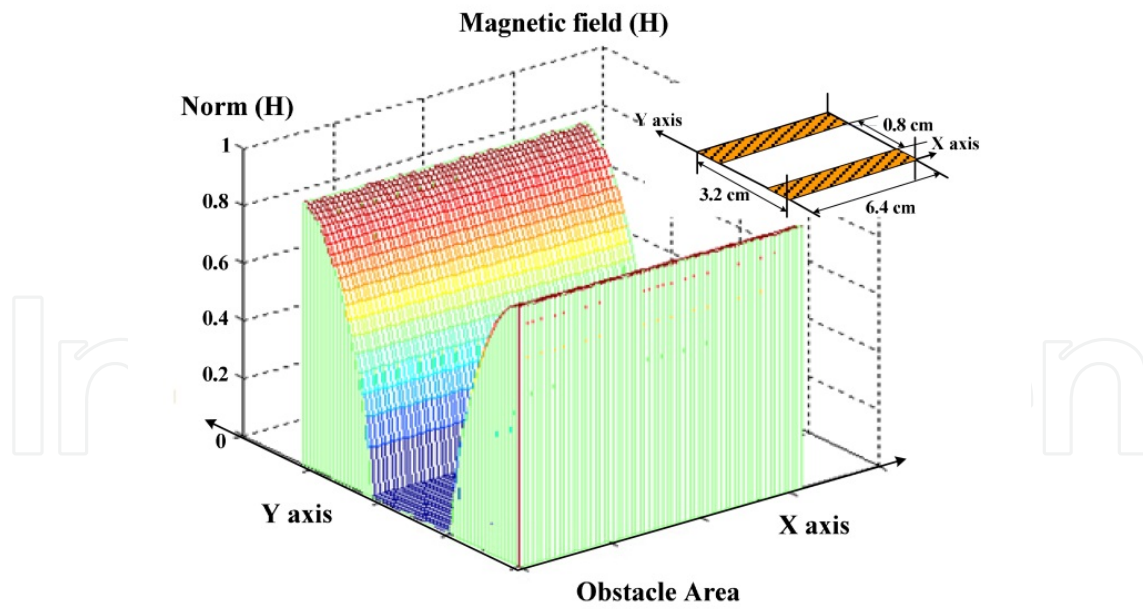
(a) Obstacle structure ratio of $d/a = 0.25$ (b) Obstacle structure ratio of $d/a = 0.125$

Figure 14. Comparison of dB(S11), dB(S21) of capacitive obstacle between the WCD and the CST simulation

Fig.14(a) presents the comparison of dB(S11) and dB(S21) of the capacitive obstacle structure between the WCD and the CST simulation. In the case of a width of obstacle structure is equal to 0.8 cm., we can obtain the -3 dB cutoff frequency at 3.43 GHz. Fig.14(b) presents the comparison of dB(S11) and dB(S21) of capacitive obstacle structure between The WCD and the CST simulation, of the obstacle structure width equal to 0.4 cm. We can obtain the -3 dB cutoff frequency at 4.82 GHz. This comparison revealed good agreement. We observed that the shunt capacitive circuit is presented as a low pass filter.



(a) Electric field



(b) Magnetic field

Figure 15. (a) The 2.5D electromagnetic field illustration

Fig.15 shows the 2.5D normalized electromagnetic field distributions on the capacitive obstacle that are agreements with the electromagnetic field theory. The electric field density of TE_{01} fundamental mode, as shown in Fig.15(a), is minimum at the center obstacle and is maximum at the discontinuity of boundary obstacle, and we observed that the electric field on the conducting surface is null. In Fig.15(b), the amplitude of magnetic field on the both sides of the conducting surface in y direction is maximal and decreases until to zero at the obstacle internal edges.

5.3. Rectangular window analysis

Finally, we study the rectangular window with a width of window equal to 0.9 cm. and a height equal to 0.675 cm., then we compare the analyzed results between the WCD and the CST simulation. The rectangular window section in the waveguide transforms the LC shunt parallel resonant circuit, as shown in Fig.16. We use the dimensions of rectangular waveguide consisting of a width (a) equal to 2.4 cm., a height (b) equal to 1.8 cm., the rectangular window dimensions are determine as in Fig.16. The cutoff frequency of the waveguide is 6.25 GHz. After simulating by the WCD tool, the input reactance of the rectangular window can be obtained at a resonant frequency of 15.5 GHz. An example of the reactance variation on the WCD display window is shown in Fig.17.

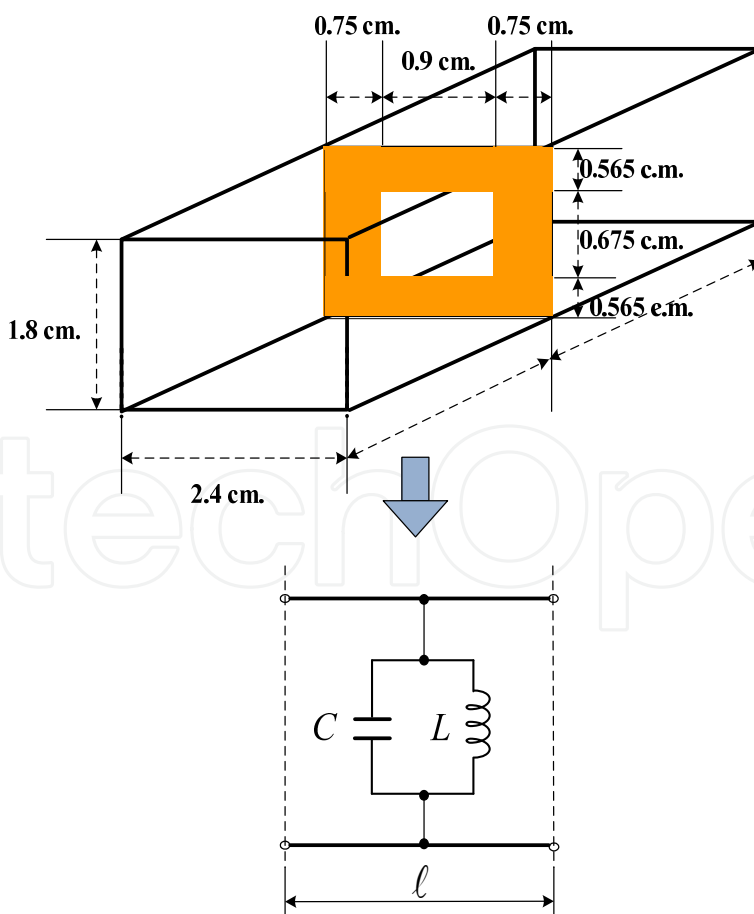


Figure 16. (a) The rectangular window structure

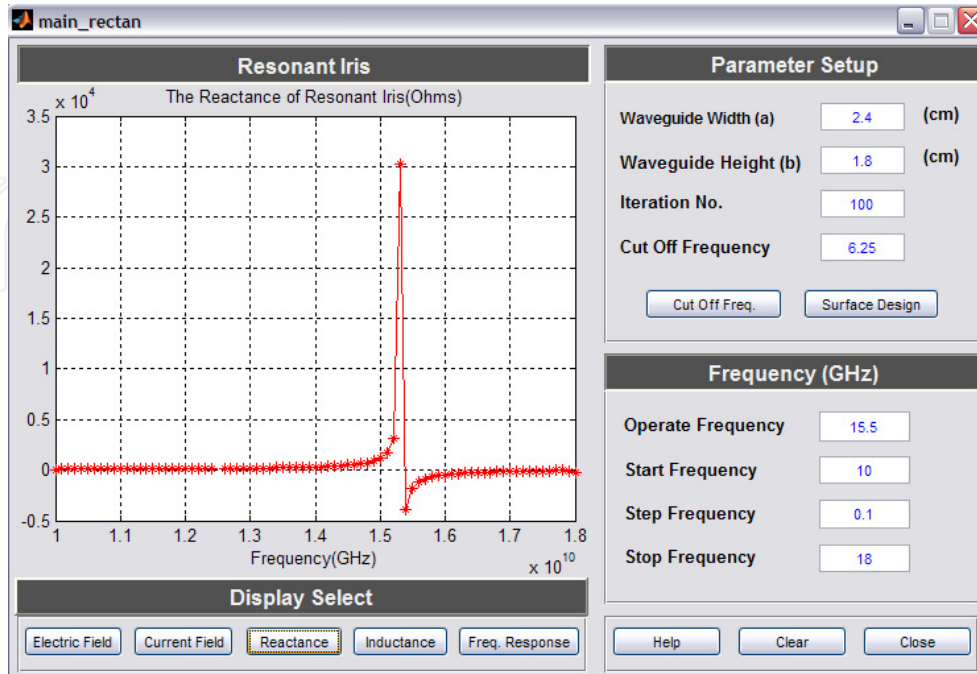


Figure 17. The reactance of rectangular window

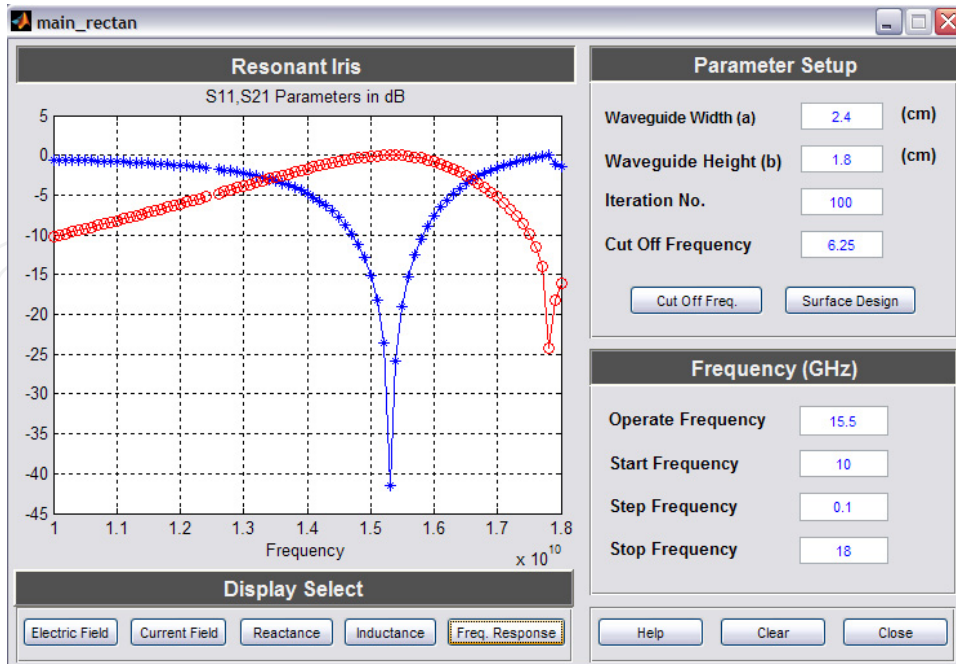
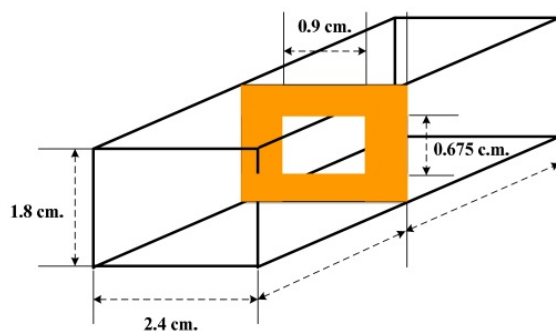


Figure 18. The dB(S11) and dB(S21) parameters of rectangular window

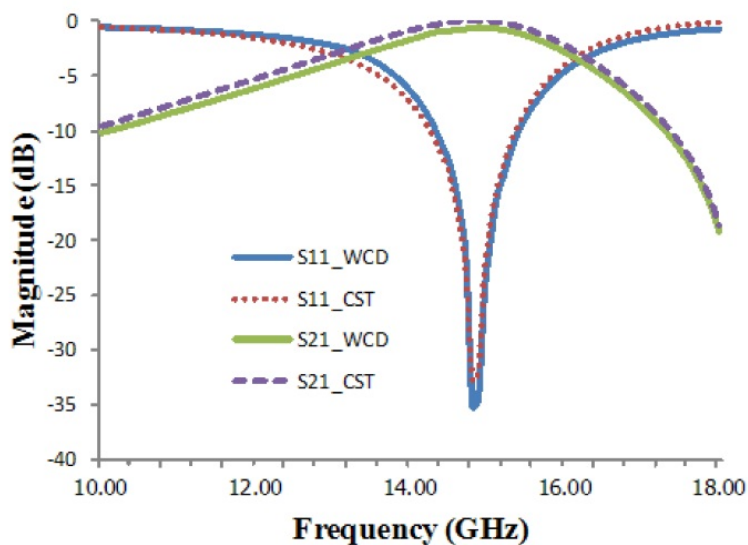
Fig.18 shows the $\text{dB}(S_{11})$ and $\text{dB}(S_{21})$ parameters of the operating frequency of 10-18 GHz, the rectangular windows is presented as a band pass filter, the -3 dB lower and upper cutoff frequency is at 15.25 GHz and at 16.12 GHz respectively. We observed that the center frequency is equal to 11 GHz and the bandwidth is equal to 2.98 GHz.

Fig.19 presents the comparison of $\text{dB}(S_{11})$ and $\text{dB}(S_{21})$ of the rectangular obstacle structure between the both simulations, we can obtain the -3 dB lower cutoff frequency at 13.25 GHz. and -3 dB upper cutoff frequency at 16.35 GHz. This comparison revealed good agreement.

We observed that the equivalent circuit at the resonant frequency is a shunt LC circuit.

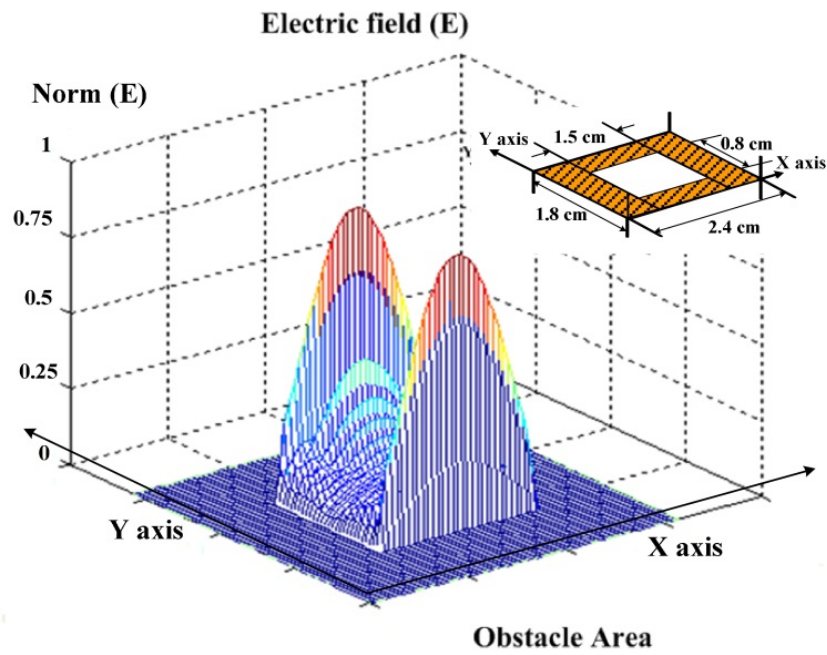


(a) Rectangular obstacle structure

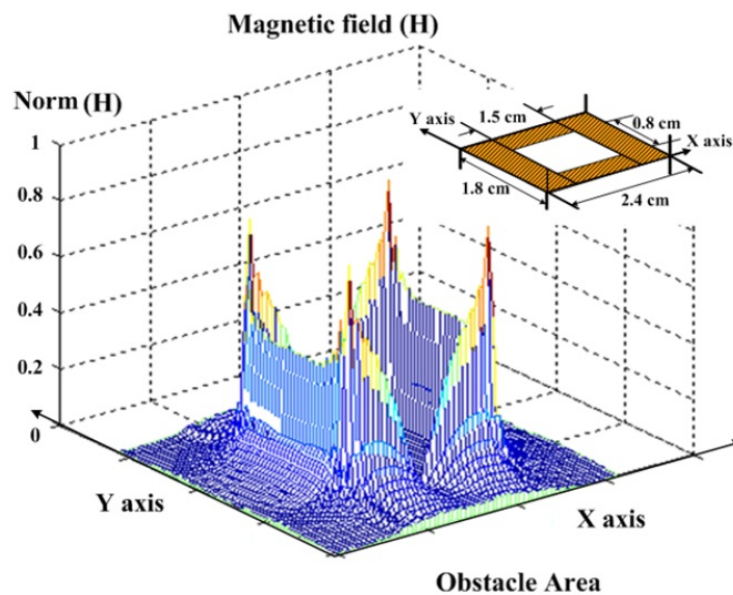


(b) Comparison of $\text{dB}(S_{11})$, $\text{dB}(S_{21})$ of rectangular obstacle between the WCD and CST simulation

Figure 19. (a) The rectangular obstacle structure and the comparison of $\text{dB}(S_{11})$, $\text{dB}(S_{21})$ of rectangular obstacle between the WCD and CST simulation



(a) Electric field



(b) Magnetic field

Figure 20. (a) The 2.5D electromagnetic field illustration

Fig.20 shows the 2.5D electric and current distributions of TE₀₁ fundamental mode on the rectangular window which are agreements with electromagnetic field theory. In Fig.20 (a), the normalized electric field peak is at the obstacle edge in x direction and minimum values are at the rectangular center window. In Fig.20(b), most current density distributions are presented at around conducting edge. The field density distribution can be used to lean qualitatively about the obstacle's operating behavior.

For efficiency of calculation, the computation time of the WCD simulation depends on the EM algorithm associating a pixel of obstacle structure to a class in an iterative process. In this simulation, the calculation at the 10 frequencies steps with 32×64 of cell numbers and 1 mm. of cell size will be equal to approximately 45 seconds of computing time, which is less than 2 times of the CST simulation (run on Pentium IV Processor, 1 GB of RAM at 3.0 GHz of speed).

6. Conclusion

The capability of developed WCD simulation based on the Wave Iterative Method (WIM) has been presented to the complex description of the 2.5D electromagnetic field and the characteristic analysis of the obstacle structures. The WCD simulation is properly conceived to apply for the inductive and the capacitive element in the rectangular waveguide without resorting to extensive computation times; it appears as an efficient alternative to the CST simulation. In the case of wave propagation, the WCD simulation can use shown the electromagnetic field distributions on the conducting obstacle. In conclusion, the WCD simulation can be used in the waveguide lumped circuit analysis and has proven to be with high accuracy and efficacy a useful tool for microwave circuit design and an educational aid.

Author details

Somsak Akatimagool and Saran Choocadee

Department of Teacher Training in Electrical Engineering,

King Mongkut's University of Technology North Bangkok, Thailand

Acknowledgement

The authors would like to thank the Faculty of Technical Education, Rajamangala University of Technology Thanyaburi, Thailand, for providing the CST Microwave Studio® software for data analysis.

7. References

- [1] T. Hiraoka, C. P. Chen, T. Anada, J. P. Hsu, Z. W. Ma, and C. C. Christopoulos, "Electric Field Distributions in Microwave Planar Circuits by Small Coaxial Probe and Comparison with FDTD Method," in *Microwave Conference, European*, pp.269-272, 2005.
- [2] J. W. Bandler, A. S. Mohamed, and M. H. Bakr, "TLM-based Modeling and Design Exploiting Space Mapping," *Microwave Theory and Techniques, IEEE Transactions on*, vol.53, pp. 2801-2811, 2005.
- [3] S. Seunghyun, K. Hyeong-Seok, J. Hyun-Kyo, and M. Un-Chul, "Frequency Domain Analysis of Microstrip Filters and Antennae using an Adaptive Frequency Sampling Moment Method," *Magnetics, IEEE Transactions on*, vol.42, pp.607-610, 2006.

- [4] V. K. Chaudhary, P. Verma, and U. Balaji, "Field Theory Based CAD of Inductive Iris Waveguide Filter," in Asia-Pacific Microwave Conference, APMC 2001, vol.1, pp.318-321, 2001.
- [5] A. Sallier, J. Bornemann, and W. J. R. Hoefer, "Field-Based Waveguide Filter Synthesis in the Time Domain," AEU - International Journal of Electronics and Communications, vol.57, pp.119-127, 2003.
- [6] I. C. Hunter, L. Billonet, B. Jarry, P. Guillon, "Microwave Filters-Applications and Technology", Microwave Theory and Techniques, IEEE Transactions on, vol.50, pp. 794 – 805, 2002.
- [7] Y. P. Zhang, H. Guorui, Z. Wenmei and J. H. Sheng, "Electromagnetic Mode Theory of Periodically-Loaded Oversized Imperfect Waveguide and its Application to the Propagation of Radio Waves in Long Wall Coal Mining Face Tunnels", Antennas and Propagation, IEEE Transactions on, vol.58, no.5, pp.1816-1822, 2010.
- [8] N.Marcuvitz, "Waveguide Handbook", Short Run Press Ltd., London, UK, 1986.
- [9] S. Akatimagool, D. Bajan, and H. Baudrand, "Analysis of Multi-layer Integrated Inductors with Wave Concept Iterative Procedure (WCIP)," in Microwave Symposium Digest, 2001 IEEE MTT-S International, vol.3, pp.1941-1944, 2001.
- [10] S. Khamkleang and S. Akatimagool, "Microwave Planar Circuit Design Tool in the teaching of Microwave Engineering," in Electrical Engineering/Electronics, Computer, Telecommunications and Information Technology, ECTI-CON 2009, 6th International Conference on, pp.830-833, 2009.
- [11] S. Choocadee and S. Akatimagool, "Development of Efficiency EM Simulation Tool for Capacitive and Inductive Obstacle Analysis," in Electrical Engineering/Electronics Computer Telecommunications and Information Technology (ECTI-CON), International Conference on, pp.1154-1158, 2010.
- [12] H.Baudrand,"Introduction of Microwave Circuit ", Toulouse, France, 1993.